

Differences in subependymal vein anatomy may predispose preterm infants to GMH–IVH

Domenico Tortora,¹ Mariasavina Severino,¹ Mariya Malova,² Alessandro Parodi,² Giovanni Morana,¹ Jan Sedlacik,³ Paul Govaert,^{4,5} Joseph J Volpe,⁶ Andrea Rossi,¹ Luca Antonio Ramenghi²

► Additional material is published online only. To view please visit the journal online (<http://dx.doi.org/10.1136/archdischild-2017-312710>)

¹Neuroradiology Unit, Istituto Giannina Gaslini, Genoa, Italy
²Neonatal Intensive Care Unit, Istituto Giannina Gaslini, Genoa, Italy

³Department of Neuroradiology, University Medical Center Hamburg-Eppendorf (UKE), Hamburg, Germany

⁴Section of Neonatology, Department of Pediatrics, Sophia Children's Hospital, Erasmus MC, University Medical Center Rotterdam, Rotterdam, The Netherlands

⁵ZNA Koningin Paola Kinderziekenhuis, Antwerp, Belgium

⁶Department of Neurology, Boston Children's Hospital and Harvard Medical School, Boston, Massachusetts, USA

Correspondence to

Dr Andrea Rossi, Neuroradiology Unit, Istituto Giannina Gaslini, Via Gerolamo Gaslini, 16147 Genoa, Italy; andrearossi@gaslini.org

Received 15 January 2017

Revised 26 April 2017

Accepted 27 April 2017

ABSTRACT

Background and purpose The anatomy of the deep venous system plays an important role in the pathogenesis of brain lesions in the preterm brain as shown by different histological studies. The aims of this study were to compare the subependymal vein anatomy of preterm neonates with germinal matrix haemorrhage–intraventricular haemorrhage (GMH–IVH), as evaluated by susceptibility-weighted imaging (SWI) venography, with a group of age-matched controls with normal brain MRI, and to explore the relationship between the anatomical features of subependymal veins and clinical risk factors for GMH–IVH.

Methods SWI venographies of 48 neonates with GMH–IVH and 130 neonates with normal brain MRI were retrospectively evaluated. Subependymal vein anatomy was classified into six different patterns: type 1 represented the classic pattern and types 2–6 were considered anatomic variants. A quantitative analysis of the venous curvature index was performed. Variables were analysed by using Mann-Whitney U and χ^2 tests, and a multiple logistic regression analysis was performed to evaluate the association between anatomical features, clinical factors and GMH–IVH.

Results A significant difference was noticed among the six anatomical patterns according to the presence of GMH–IVH ($\chi^2=14.242$, $p=0.014$). Anatomic variants were observed with higher frequency in neonates with GMH–IVH than in controls (62.2% and 49.6%, respectively). Neonates with GMH–IVH presented a narrower curvature of the terminal portion of subependymal veins ($p<0.05$). These anatomical features were significantly associated with GMH–IVH ($p<0.05$).

Conclusion Preterm neonates with GMH–IVH show higher variability of subependymal veins anatomy confirming a potential role as predisposing factor for GMH–IVH.

INTRODUCTION

Germinal matrix haemorrhage–intraventricular haemorrhage (GMH–IVH) is one of the main complications of prematurity, with important effects on morbidity, mortality and long-term neurological outcome.¹ In particular, severe GMH–IVH is associated with increased short-term and long-term neurological morbidity,² while the long-term neurological outcome of milder form of GMH–IVH is still debated and remains an active area of research.³ Several studies addressed epidemiology, pathogenesis and risk factors of this multifactorial disease⁴ demonstrating that lower gestational age is the most

What is already known on this topic?

- Germinal matrix haemorrhage–intraventricular haemorrhage (GMH–IVH) is one of the main complications of prematurity, with important effects on mortality and long-term neurological outcome.
- Several risk factors have been identified, such as the gestational age, absent antenatal steroid treatment, low Apgar scores or pneumothorax.

What this study adds?

- Preterm neonates with GMH–IVH presented a higher variability of the subependymal veins anatomy, including a narrower curvature, when compared with infants without GMH–IVH.
- Variations of subependymal veins anatomy may be additional independent predisposing factors for GMH–IVH.

important factor for the development of GMH–IVH. However, absent antenatal steroid treatment, low Apgar scores, pneumothorax, early sepsis,⁵ inherited thrombophilia⁶ and the use of inotropic drugs during the first days of life may contribute to GMH–IVH. Despite continuous improvement of perinatal care produced a significant reduction of these acquired risk factors,^{7–10} the incidence of GMH–IVH has not changed accordingly, thus highlighting the importance of structural and connatal factors.¹¹

Interestingly, histological studies have provided some evidence that the anatomy of the subependymal veins (SVs) may also be implicated in the pathogenesis of GMH–IVH.^{12–14} In particular, it has been hypothesised that the peculiar ‘U-turn’ shape of the terminal vein may alter blood drainage through the SV near the caudathalamic groove, determining an increase of venous pressure in periventricular zones and germinal matrix leading to GMH–IVH.¹³ However, this not recent but very intriguing hypothesis remains unsubstantiated, since the potential role of deep venous anatomy as a contributing factor to GMH–IVH has not been systematically explored so far.

Recently, the development of MR susceptibility-weighted imaging (SWI venography) has allowed the in vivo depiction of small veins without the



CrossMark

To cite: Tortora D, Severino M, Malova M, et al. *Arch Dis Child Fetal Neonatal Ed* Published Online First: [please include Day Month Year]. doi:10.1136/archdischild-2017-312710

Original article

need of a contrast agent¹⁵ and, additionally, has enhanced diagnostic sensitivity in assessment of low-grade brain haemorrhages of neonates.¹⁶

The aims of this study were to use SWI venography to define the features of SV anatomy in preterm neonates with GMH–IVH and to compare the SV anatomy of preterm neonates with GMH–IVH with a group of age-matched controls with normal brain MRI. Moreover, the relationships between SV anatomy, GMH–IVH and clinical characteristics were assessed.

MATERIALS AND METHODS

Subjects

For the current study, all very-low-birth-weight preterm neonates (birth weight <1500 g) who underwent brain MRI between April 2012 and March 2015 at term equivalent age as a part of a screening programme for identification of prematurity-related lesions were retrospectively identified. According to the modified Papile classification, GMH–IVH were classified in: (1) grade 1, when the haemorrhage was restricted to the germinal matrix, (2) grade 2, when they were extended into the lateral ventricles, occupying <50% of the ventricular volume, (3) grade 3, when they were characterised by larger amounts of intraventricular blood causing hydrocephalus and (4) grade 4, when they were complicated by haemorrhagic venous infarction in the periventricular white matter.² Neonates were then divided into two groups: (1) with GMH–IVH and (2) with normal brain MRI. Four exclusion criteria were used in this study: (1) presence of dilated lateral ventricles with distorted SV morphology, related to either posthaemorrhagic hydrocephalus or large periventricular venous infarct, (2) presence of a large intraventricular blood clot hampering the detection of the SV course on the SWI venography, (3) absence of SWI venography in the study protocol and (4) poor quality of MR images.

Imaging

All MRI studies were performed in the Neuroradiology Unit of the Gaslini Children Hospital on a 1.5T scanner, using a dedicated neonatal 8-channel head coil. All patients were fed before MRI examination in order to achieve spontaneous sleep. Hearing protection was used in all patients. Heart rate and oxygen saturation were non-invasively monitored by pulse-oximetry during

examination. All neonates underwent the same MRI protocol (see online supplementary table 1).

Analysis of SWI venography

MR Images analysis was performed in three different phases.

Phase 1: a paediatric neuroradiologist with 25 years of experience in neonatal neuroimaging reviewed all MRI studies using a workstation equipped with a professional DICOM viewer (OsiriX Imaging Software; <http://www.osirix-viewer.com>) in order to perform an image-quality assessment of the acquired SWI sequences, evaluating the general image quality, noise, venous contrast and the presence of motion artefacts. Furthermore, the same reader identified neonates with normal brain MRI and with GMH–IVH and excluded SWI venography studies burdened with large intraventricular blood clot and with expanded ventricles.

Phase 2: two neuroradiologists (with 10 and 7 years of experience, respectively), blinded to neonate identity, reviewed independently the SWI sequences selected in phase 1. SVs were evaluated on axial-reformatted SWI slices for each brain hemisphere. Based on their anatomical location, the following veins were identified: (1) the anterior septal vein (ASV), (2) the thalamostriate vein (TSV), (3) the direct lateral vein (DLV), (4) the atrial vein (AV) and (5) the internal cerebral vein (ICV) (figure 1). According to the classification of the SV anatomy proposed by Tortora *et al* in neonates with normal brain MRI,¹⁷ readers independently classified SV of each brain hemisphere into six patterns: type 1 was considered as the typical pattern,¹⁸ while types 2–6 reflected anatomical variations (table 1 and figure 1). Subsequently, the same two neuroradiologists jointly reviewed the SWI venography of neonates with discordant evaluation and to reach a consensus on the SV pattern classification. Moreover, we tested if the venous anatomy could be correctly identified by a less experienced radiologist, who performed the same analysis on a subgroup of 50 randomly selected cases (100 hemispheres).

Phase 3: in order to evaluate whether the ‘U-turn’ shape of the SV close to the caudate-thalamic groove is associated to GMH–IVH, a quantitative measurement of the SV curvature was performed. Such measurement was performed on the TSV in brain hemispheres with the type 1, 2 and 5 anatomical patterns. In type 3 and 4 patterns, the curvature degree was measured on

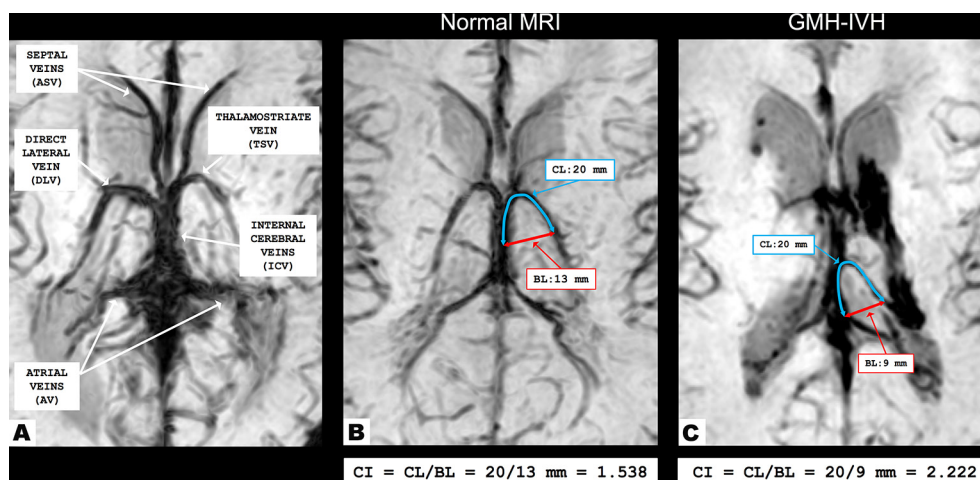


Figure 1 (A) Representation of SV on axial-reformatted SWI venography. (B and C) Axial-reformatted SWI venographies in preterm neonates with normal brain MRI (CI measurement performed on TSV) and GMH–IVH (CI measurement performed on DLV), respectively. BL, basal line; CI, curvature index; CL, curve line; GMH–IVH, germinal matrix haemorrhage–intraventricular haemorrhage; SV, subependymal vein; SWI, susceptibility-weighted imaging; TSV, thalamostriate vein.

Table 1 Characteristics of the SV patterns

SV pattern	Description
Type 1	The ASV joined the ICV at the level of the foramen of Monro and the TSV–ICV junction. The DLV was absent.
Type 2	The ASV joined the ICV posterior to both the TSV–ICV junction and the foramen of Monro, resulting in a narrower curvature of terminal portion of the TSV. The DLV was absent.
Type 3	The ASV joined the ICV close to the site of DLV–ICV junction, posterior to the foramen of Monro. The TSV was absent.
Type 4	The ASV joined the ICV posterior to both the foramen of Monro and DLV–ICV junction, resulting in a narrower curvature of terminal portion of the DLV. The TSV was absent.
Type 5	Both the TSV and DLV were present.
Type 6	Both the TSV and DLV were absent.

ASV, anterior septal vein; DLV, direct lateral vein; ICV, internal cerebral vein; SV, subependymal vein; TSV, thalamostriate vein.

the DLV. Neonatal hemispheres presenting the type 6 pattern were excluded from this part of the analysis, since both the TSV and DLV were absent. The same two neuroradiologists traced in consensus a contour line (CL) of 20 mm along the vein, focusing on the centre of its curved portion, using the segmented line function of MIPAV (Medical Image Processing, Analysis & Visualization V.7.2.0, www.mipav.cit.nih.gov). Then, a straight basal line (BL) connecting the end points of CL was drawn. Vein curvature was quantified using the curvature index (CI) defined by the ratio between CL and BL.¹⁹ Higher values of CI correspond to a narrower curved morphology of the SV (figure 1B–C). Measurements were repeated three times, and the mean of these values was used for statistical analysis.

In order to validate the method of CI measurement, results of the phase 3 analysis were compared with a second set of measurements performed by the same two neuroradiologists and by a less experienced radiologist on the same smaller randomly selected group of 50 neonates (100 brain hemispheres).

Clinical data

Demographic and anthropometric characteristics (gender, birth weight and gestational age), antenatal history (twin gestation, intrauterine growth restriction and antenatal steroids dosage), perinatal variables (type of delivery, and Apgar score) and clinical course (respiratory distress syndrome, need for inotropic treatment during first 3 days of life, pneumothorax and patient ductus arteriosus) were recorded for all neonates (see online supplementary table 2).

Statistical analysis

Statistical analysis was performed by using SPSS Statistics for Mac, V.21.0. The level of significance was set at $p < 0.05$. Differences between continuous variables were evaluated by Student's t-test and Mann-Whitney U test, while categorical variables were compared by using χ^2 test. Cohen's kappa coefficient was calculated to test inter-rater agreement. Multivariable logistic regression models were used to determine clinical and anatomical factors that were independently associated with GMH–IVH. All variables that were hypothesised to be associated with GMH were entered into the nominal logistic model and then a backward elimination was used to remove nonsignificant independent factors ($p > 0.05$). In order to evaluate the reproducibility of the quantitative evaluation of CI, a Bland-Altman plot analysis was performed comparing three sets of CI measurements.

The institutional review board approved this retrospective study, and the parents provided written informed consent.

RESULTS

Subjects

The brain MRI studies of 248 consecutive preterm neonates acquired from April 2012 and March 2015 were retrospectively evaluated. The MRI studies of 70 patients were excluded based on the criteria mentioned above. In particular, 24 neonates presented dilated lateral ventricles (19 posthaemorrhagic hydrocaephalus and five large periventricular venous infarcts) or large intraventricular blood clot that masked the SV on the SWI venography, 26 studies were affected by motion artefacts, and in the remaining 20, no SWI venography was performed for technical reasons.

Thus, the MRI studies of 178/248 (71.7%) preterm neonates were included in the study. Forty-eight (27%, 48/178) presented GMH–IVH (21 females, average gestational age 28 ± 2.83 weeks), while 130 (73%, 130/178) had a normal brain MRI (69 females, average gestational age 29.07 ± 2.00 weeks). Fourteen of 48 GMH–IVH neonates presented unilateral haemorrhage (eight exclusively in the left side). Accordingly, 82 GMH–IVH hemispheres (42 left) and 274 normal hemispheres (136 left) were considered for analysis (figure 2).

Qualitative analysis of the SV

The consensus reading was necessary in 4/356 (1%) neonatal hemispheres (K coefficient=0.996; $p=0.001$). In all discordant cases, the consensus reading was required to define the site of ASV–ICV junction in order to distinguish type 3 and type 4 patterns (3/4 hemispheres were finally assigned to the type 3 pattern).

The frequencies and percentages of SV anatomical patterns for each group of neonates are reported in table 2. A significant difference was noticed between the six anatomical patterns according to the presence of GMH–IVH ($\chi^2=14.242$, $p=0.014$). The classic anatomical pattern was more frequent in neonates with normal brain MRI (50.4%) than in neonates with GMH–IVH (37.8%) ($p=0.014$). Anatomic variants (type 2–6) were observed with higher frequency in neonates with GMH–IVH than those with normal brain MRI (62.2% and 49.6%, respectively). No left-to-right differences were observed ($p > 0.05$). In the 14 infants with unilateral GMH–IVH, the venous anatomy on the affected side was characterised by presence of anatomical variations (type 2–6 patterns) in 12/14 cases. In the contralateral normal hemispheres, we found the classic type 1 pattern in 13/14 cases. Therefore, differences in the venous anatomy between the affected and normal hemispheres were overall found in 13/14 cases.

Finally, there was a good agreement between the analysis performed by the paediatric neuroradiologists and the less experienced radiologist (K coefficient=0.812; $p=0.001$). All discordant cases (6/100) regarded the distinction between type 3 and type 4 patterns.

Quantitative analysis of the SV curvature

The assessment of the CI was performed on TSV in 197 hemispheres (39 GMH–IVH) and on DLV in 131 hemispheres (30 GMH–IVH). Twenty-eight out of 356 hemispheres with type six pattern were excluded from the quantitative analysis, because TSV and DLV are absent in this pattern. No significant differences were observed between mean CI of TSV and DLV ($p=0.320$).

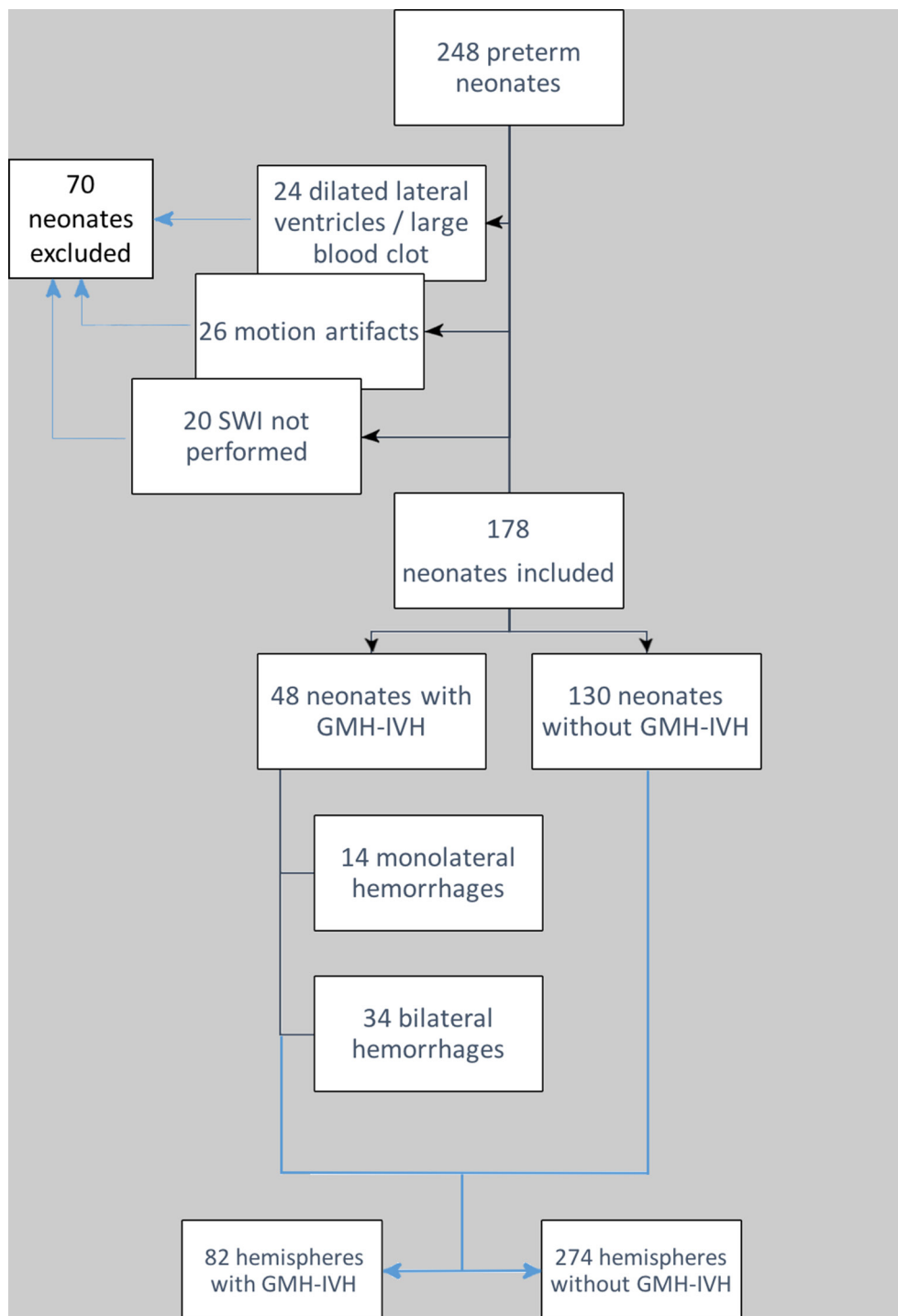


Figure 2 Study population flowchart. GMH-IVH, germinal matrix haemorrhage–intraventricular haemorrhage.

Mean CI of both TSV and DLV was significantly higher in neonates with GMH-IVH both in the left (1.651 ± 0.374 vs 1.422 ± 0.249 for TSV, and 1.681 ± 0.332 vs 1.425 ± 0.338 for DLV) and right hemisphere (1.423 ± 0.274 vs 1.384 ± 0.255 for TSV, and 1.590 ± 0.167 vs 1.384 ± 0.266 for DLV) (table 3).

Bland-Altman plot analysis did not show significant differences in the two sets of CI measurements performed on the group of 50 randomly selected neonates by two expert neuroradiologists and by the couple of expert and less experienced readers, respectively (mean difference -0.003 ; SD 0.081 ; 95% CI -0.0192 to 0.013 ; $p=0.709$, and mean difference -0.052 ;

SD 0.035 ; 95% CI -0.0182 to 0.032 ; $p=0.542$, respectively) (see online supplementary result 1).

Relationship between clinical data, venous anatomy and GMH-IVH

To compare the relationship of both the anatomical features of SV and clinical data with GMH-IVH, we performed a multiple logistic regression analysis considering qualitative and quantitative metrics used to evaluate the SV anatomy and all clinical records as independent factors. Independent variables that

Table 2 Results of SWI venography qualitative analysis

Qualitative overall analysis	No GMH-IVH		GMH-IVH		p	
Type 1	138 (50.4%)		31 (37.8%)			
Type 2	9 (3.3%)		6 (7.3%)			
Type 3	85 (31.0%)		27 (32.9%)			
Type 4	16 (5.8%)		3 (3.7%)			
Type 5	11 (4.0%)		2 (2.4%)			
Type 6	15 (5.5%)		13 (15.9%)			
TOTAL (hemispheres)	274		82		0.014	
Qualitative right-to-left analysis	Right	Left	Right	Left	p No GMH-IVH	p GMH-IVH
Type 1	79(57.2%)	59(43.4%)	20(50.0%)	11(26.2%)		
Type 2	3 (2.2%)	6 (4.4%)	4 (10.0%)	2 (4.8%)		
Type 3	37 (26.8%)	48 (35.3%)	7 (17.5%)	20 (47.6%)		
Type 4	5 (3.6%)	11 (8.1%)	1 (2.5%)	2 (4.8%)		
Type 5	6 (4.3%)	5 (3.7%)	1 (2.5%)	1 (2.5%)		
Type 6	8 (5.8%)	7 (5.1%)	7 (17.5%)	6 (14.3%)		
TOTAL (hemispheres)	138	136	40	42	0.173	0.078

GMH-IVH, germinal matrix haemorrhage-intraventricular haemorrhage; SWI, susceptibility-weighted imaging.

resulted significantly associated to GMH-IVH are reported in [table 4](#). GMH-IVH was significantly associated with both the SV anatomical pattern (OR=2.47, p=0.0164) and CI (right CI: OR=4.202, p=0.0003; left CI: OR=2.044, p=0.0227).

DISCUSSION

The vascular site of origin of GMH-IVH appears to be the prominent endothelial-lined vessels, not clearly arterial or venous, in the germinal matrix.^{12 20–22} The relative importance of the arterial or venous side of this microcirculation is not fully elucidated. Importance for the role of the venous vascularisation was raised by the studies of Takashima *et al*,²³ who described for the first time the retrograde venous drainage of the germinal matrix and demonstrated that GMH-IVH occurs at the border zone between the germinal matrix and the adjacent cerebral parenchyma, at the site where germinal matrix venules converge to join the TSV.^{23 24} Indeed, the hypothesis that the morphology of the SV could play a role in the pathogenesis of GMH-IVH was originally introduced in 1964 by Larroche.¹⁴ In particular, the risk of subependymal haemorrhage was thought to be related to venous stasis and thrombosis occurring near the foramen of Monro and caudate head. The importance of the anatomy of the vein in this context was emphasised by Volpe,¹³ but to our knowledge, no systematic validation has been provided thus far. Therefore, in this study, we aimed to qualitatively and quantitatively evaluate the SV phenotype associated with GMH-IVH in preterm neonates using the non-invasive SWI venography.

Table 3 Results of SWI venography quantitative analysis

Quantitative analysis	Mean TSV CI (mean±SD)	No GMH-IVH	GMH-IVH	p
Right		1.423±0.274	1.616±0.155	0.024
Left		1.422±0.249	1.651±0.374	0.005
	Mean DLV CI (mean±SD)			
Right		1.384±0.266	1.590±0.167	<0.001
Left		1.425±0.338	1.681±0.332	0.005

CI, curvature index; DLV, direct lateral vein; GMH-IVH, germinal matrix haemorrhage-intraventricular haemorrhage; SWI, susceptibility-weighted imaging; TSV, thalmostriate vein.

Notably, we found a positive correlation between the presence of anatomical SV variants and the occurrence of GMH-IVH in preterm neonates. This association was further supported by differences in venous anatomy between the affected and normal hemispheres found in neonates with unilateral GMH-IVH, who presented SV variants in almost all affected hemispheres (86%) and the typical SV pattern in the normal sides. Of note, the presence or absence of TSV and its morphology are the key features differentiating the SV variants from the classic pattern.¹⁸ Thus, in the present study, SV variants that mainly differentiate GMH-IVH hemispheres from controls were characterised either by the absence of TSV and DLV (type 6) or by a narrow curved morphology of the TSV (type 2). Therefore, it can be postulated that the absence of both TSV and DLV may influence the venous drainage of the germinal matrix, resulting in a longer course of venules that will drain into the S more posteriorly (through the AV) ([figure 3A and B](#)). This peculiar venous drainage may increase the risk for developing venous stasis and venous thrombosis, both known risk factors for GMH-IVH. In addition, developmental immaturity in the cerebral circulation, observed at younger gestational ages due to ongoing angiogenesis and altered vasoregulatory mechanisms,^{25–28} may contribute to the occurrence of GMH-IVH.

However, we observed a higher incidence of GMH-IVH also in neonatal hemispheres with a narrower curvature of the TSV (type 2) ([figure 3C](#)). Therefore, we used a quantitative approach to investigate if the morphology of TSV or other SV could additionally influence the occurrence of GMH-IVH.¹³ Intriguingly, we found that the TSV of neonates with GMH-IVH were characterised by a higher CI of the portions preceding the anastomoses with the ICV. Recently, computational fluid dynamics has been employed to investigate the impact of the vessel curvature on blood flow.²⁹ These analyses showed that increased vessel curvature leads to flow alterations and increased lumen shear stress that determine venous thrombosis proportionally to the curvature degree.³⁰ Therefore, we suppose that the narrower curvature of the terminal portion of TSV may cause blood flow alterations and blood congestion in the germinal matrix venular system with a retrograde mechanism, leading to increased pressure on the immature vessel walls and higher risk of venous rupture.²⁷ This hypothesis is further supported by the

Table 4 Logistic regression analysis results

Independent factors	Coefficient	SE	OR	95% CI	p
Right CI	4.202	1.163	6.82	2.82–10.76	0.0003
Left CI	2.044	0.897	7.72	1.22–44.84	0.0227
SV anatomical pattern	1.296	0.581	2.47	0.85–7.14	0.0164
Gestational age	−0.366	0.121	0.69	0.54–0.88	0.0027
Early pneumothorax	2.174	1.098	8.79	1.02–75.75	0.0478
Early hypotension	1.922	0.811	6.83	1.39–33.56	0.0179
Absent/incomplete prenatal steroids administration	1.238	0.587	3.45	1.09–10.91	0.0351

CI, curvature index; SV, subependymal veins.

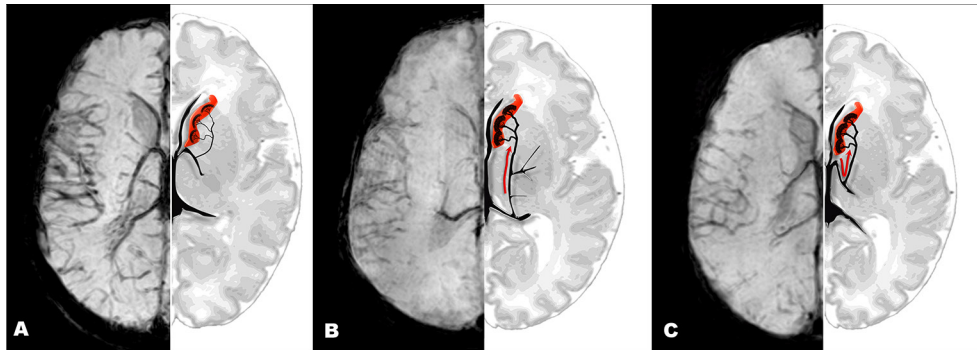


Figure 3 Axial-reformatted SWI venographies and corresponding schematic representations of SV patterns and venous drainage of the germinal matrix near the caudothalamic groove. (A) Classic anatomical pattern. (B) Anatomical variant of subependymal vein (type 6): the ASV joins posteriorly the AV; the TSV and DLV are absent. Red arrow indicates blood congestion into the SV and the germinal matrix venous drainage. (C) Anatomical variant of subependymal vein (type 2) with narrower curvature of the TSV near the caudothalamic groove. Red arrow indicates blood congestion into the SV and the germinal matrix venous drainage.

well-known correlation between deep venous thrombosis and GMH–IVH, due to a secondary increase of venous pressure in the germinal matrix veins.^{31 32}

Several clinical conditions altering the cerebral circulation in the preterm may lead to increase venous pressure at different levels of the venous system and, accordingly, promotes the occurrence of GMH–IVH. In particular, the respiratory and haemodynamic instability caused by such preterm birth complications (as early pneumothorax or arterial hypotension) may result in wide fluctuations of cerebral blood flow, due to an impaired mechanism of cerebral blood flow autoregulation and disturbances in the venous circulation.^{4 26} A clear relation among GMH–IVH, pneumothorax and arterial hypotension is well established. Moreover, it has been demonstrated that protection against cerebrovascular events in preterm neonates can be provided by prenatal administration of glucocorticoid, which decreases the severity of the respiratory distress and the incidence of GMH–IVH³³ and stabilises the existing germinal matrix vasculature.³⁴ Consistent with these studies, our multivariable logistic regression analysis demonstrated an association of GMH–IVH with pneumothorax, arterial hypotension and incomplete prenatal steroid administration.⁶

Taken together, these observations support the hypothesis that the vascular architecture of SV may play a role in the pathogenesis of GMH–IVH, particularly when clinical conditions affecting the cerebral circulation occur. Nevertheless, the causality between morphology of the SV and the occurrence of GMH–IVH remains speculative and is worthy of future investigation, both in animal models and in human infants.

Among the limitations of this study, we are aware that the neuroradiologists who performed the image analysis were not

blinded to the presence or absence of GMH–IVH, easily recognisable on the same SWI venography sequence. Another limit is that we were obliged to exclude a relatively high number of neonates with GMH–IVH (ie, 24 cases), thus potentially lowering the statistical power of the analysis. Moreover, we could not evaluate the SV anatomy in preterm neonates with severe GMH–IVH consisted with ventricular dilatation, large intraventricular blood clots and/or venous infarcts, as they deeply ruin normal venous anatomy. This point could be addressed in future prospective studies using ultrasound with Doppler to evaluate the SV anatomy in the immediate postnatal period, before the occurrence of GMH–IVH. Indeed, new 3D and 4D ultrafast Doppler techniques with extremely high resolution for very small brain vessels have been developed and applied in small animal models, and their promising clinical application is on the horizon.³⁵

CONCLUSIONS

MR SWI venography represents an *in vivo*, non-invasive method able to describe morphological, positional and numerical variants of SV associated to GMH–IVH in preterm neonates. Anatomical features of SV may be important predisposing factors for GMH–IVH when clinical conditions affecting the cerebral blood flow occur in the preterm brain.

Contributors DT conceptualised and designed the study, drafted the manuscript, performed statistical analysis and approved the final manuscript as submitted. MS, MM, AP, GM and JS conceptualised the study, implemented the imaging sequence and venographic image reconstruction method, carried out the initial analysis, reviewed and revised the manuscript and approved the final manuscript as submitted. PG and JIV conceptualised the study, critically reviewed the manuscript and approved the final manuscript as submitted. AR and LAR conceptualised the

study, coordinated and supervised data collection, critically reviewed the manuscript and approved the final manuscript as submitted.

Funding This research was supported by the Eu-Brain non-profit association.

Competing interests None declared.

Ethics approval Gaslini Institute review board.

Provenance and peer review Not commissioned; externally peer reviewed.

© Article author(s) (or their employer(s) unless otherwise stated in the text of the article) 2017. All rights reserved. No commercial use is permitted unless otherwise expressly granted.

REFERENCES

- Ramenghi LA. Germinal Matrix-Intraventricular haemorrhage: still a very important brain lesion in premature infants!. *J Matern Fetal Neonatal Med* 2015;28:2259–60.
- Mukerji A, Shah V, Shah PS. Periventricular/Intraventricular hemorrhage and neurodevelopmental outcomes: a Meta-analysis. *Pediatrics* 2015;136:1132–43.
- Payne AH, Hintz SR, Hibbs AM, Walsh MC, Vohr BR, Bann CM, Wilson-Costello DE. Neurodevelopmental outcomes of extremely Low-Gestational-Age neonates with Low-Grade Periventricular-Intraventricular hemorrhage. *JAMA Pediatr* 2013;167:451–9.
- Ballabh P. Pathogenesis and prevention of intraventricular hemorrhage. *Clin Perinatol* 2014;41:47–67.
- Linder N, Haskin O, Levit O, et al. Risk factors for intraventricular hemorrhage in very low Birth Weight Premature Infants: a retrospective Case-Control Study. *Pediatrics* 2003;111:e590–5.
- Ramenghi LA, Fumagalli M, Groppo M, et al. Germinal Matrix Hemorrhage: intraventricular hemorrhage in Very-Low-Birth-Weight Infants: the Independent role of inherited Thrombophilia. *Stroke* 2011;42:1889–93;42:1889–93.
- Burstein J, Papile LA, Burstein R. Intraventricular hemorrhage and hydrocephalus in premature newborns: a prospective study with CT. *AJR Am J Roentgenol* 1979;132:631–5.
- Batton DG, Holtrop P, DeWitte D, et al. Current gestational age-related incidence of major intraventricular hemorrhage. *J Pediatr* 1994;125:623–5.
- Horbar JD, Badger GJ, Carpenter JH, et al. Trends in mortality and morbidity for very low birth weight infants, 1991–1999. *Pediatrics* 2002;110:143–51.
- Tortora D, Panara V, Mattei PA, et al. Comparing 3T T1-Weighted sequences in identifying hyperintense punctate lesions in preterm neonates. *Am J Neuroradiol* 2015;36:581–6.
- Sannia A, Natalizia AR, Parodi A, et al. Different gestational ages and changing vulnerability of the premature brain. *J Matern Fetal Neonatal Med* 2015;28:2268–72.
- Anstrom JA, Brown WR, Moody DM, et al. Subependymal veins in premature neonates: implications for hemorrhage. *Pediatr Neurol* 2004;30:46–53.
- Volpe JJ. Intracranial hemorrhage: germinal matrix-intraventricular hemorrhage of the premature infant. Volpe JJ, ed. *Neurology of the Newborn*. 5th edn. Philadelphia: Saunders Elsevier, 2008:517–88.
- Laroché JC. Intraventricular haemorrhages in the premature infant. part I: anatomy and physiopathology. *Biol Neonat* 1964;7:26–56.
- Haacke EM, Xu Y, Cheng YC, Reichenbach JR susceptibility weighted imaging (SWI). *Magn Reson Med*. 2004;52:612–8.
- Parodi A, Morana G, Severino MS, et al. Low-grade intraventricular hemorrhage: is ultrasound good enough? *J Matern Fetal Neonatal Med* 2015;28:2261–4.
- Tortora D, Severino M, Malova M, et al. Variability of Cerebral Deep Venous System in Preterm and Term Neonates Evaluated on MR SWI Venography. *AJNR Am J Neuroradiol*. In Press. 2016;28:2144–9.
- Stein RL, Rosenbaum AE. Deep supratentorial veins. Section I Normal deep cerebral venous system. In: Newton TH, Potts DG, eds. *Radiology of the Skull and Brain, vol 2. (angiography), book 3 (veins)*. St. Louis: Mosby, 1974. 1903–98.
- Bullitt E, Gerig G, Pizer SM, et al. Measuring tortuosity of the intracerebral vasculature from MRA images. *IEEE Trans Med Imaging* 2003;22:1163–71.
- Pape KE, Haemorrhage WJS. Ischaemia and the perinatal brain. *Clin Dev Med* 1979;69/70:1-185. Hambleton G, Wigglesworth JS. *Arch Dis Child* 1976;51:651–9.
- Ghazi-Birry HS, Brown WR, Moody DM, et al. Human germinal matrix: venous origin of hemorrhage and vascular characteristics. *AJNR Am J Neuroradiol* 1997;18:219–29.
- Paneth N, Rudelli R, Kazam MW. The pathology of germinal matrix/ intraventricular hemorrhage. In: Paneth N, Rudelli R, Kazam MW, eds. *Brain damage in the preterm infant. clinics in developmental medicine, No. 131, 1 ed.* UK: LondonMac Keith Press, 1994. 23–53.
- Takashima S, Tanaka K. Microangiography and vascular permeability of the subependymal matrix in the premature infant. *Can J Neurol Sci* 1978;5:45–50.
- Nakamura Y, Okudera T, Hashimoto T. Microvasculature in germinal matrix layer: its relationship to germinal matrix hemorrhage. *Mod Pathol* 1991;4:475–80.
- Lenn NJ, Whitmore L. Gestational changes in the Germinal Matrix of the Normal Rhesus Monkey Fetus. *Pediatr Res* 1985;19:130–5.
- Brew N, Walker D, Wong FY Cerebral vascular regulation and brain injury in preterm infants. *Am J Physiol Regul Integr Comp Physiol* 2014;1;306:R773–86.
- Grunnet ML. Morphometry of blood vessels in the cortex and germinal plate of premature neonates. *Pediatr Neurol* 1989;5:12–16.
- Evans DJ, Childs AM, Ramenghi LA, et al. Levene M1 magnetic resonance imaging of the brain of premature infants. *Lancet* 1997;350:522.
- Qiao AK, Guo XL, Wu SG, et al. Numerical study of nonlinear pulsatile flow in S-shaped curved arteries. *Med Eng Phys* 2004;26:545–52.
- Liu Q, Mirc D, Fu BM. Mechanical mechanisms of thrombosis in intact bent microvessels of rat mesentery. *J Biomech* 2008;41:2726–34.
- Ramenghi LA, Gill BJ, Tanner SF, et al. Cerebral venous thrombosis, intraventricular haemorrhage and White Matter lesions in a Preterm Newborn with factor V (Leiden) Mutation. *Neuropediatrics* 2002;33:97–99.
- Kersbergen KJ, Groenendaal F, Benders MJNL, et al. The spectrum of associated brain lesions in cerebral sinovenous thrombosis: relation to gestational age and outcome. *Arch Dis Child Fetal Neonatal Ed* 2011;96:F404–F409.
- Elimian A, Garry D, Figueroa R, et al. Antenatal betamethasone compared with dexamethasone (betacode trial): a randomized controlled trial. *Obstet Gynecol* 2007;110:26–30.
- Vinukonda G, Dummula K, Malik S, et al. Effect of prenatal glucocorticoids on Cerebral Vasculature of the developing brain * Supplemental methods. *Stroke* 2010;41:1766–73.
- Demené C, Tiran E, Sieu L-A, et al. 4d microvascular imaging based on ultrafast Doppler tomography. *Neuroimage* 2016;127:472–83.



Differences in subependymal vein anatomy may predispose preterm infants to GMH–IVH

Domenico Tortora, Mariasavina Severino, Mariya Malova, Alessandro Parodi, Giovanni Morana, Jan Sedlacik, Paul Govaert, Joseph J Volpe, Andrea Rossi and Luca Antonio Ramenghi

Arch Dis Child Fetal Neonatal Ed published online June 6, 2017

Updated information and services can be found at:

<http://fn.bmj.com/content/early/2017/06/05/archdischild-2017-312710>

References

These include:

This article cites 32 articles, 8 of which you can access for free at:
<http://fn.bmj.com/content/early/2017/06/05/archdischild-2017-312710#BIBL>

Email alerting service

Receive free email alerts when new articles cite this article. Sign up in the box at the top right corner of the online article.

Notes

To request permissions go to:

<http://group.bmj.com/group/rights-licensing/permissions>

To order reprints go to:

<http://journals.bmj.com/cgi/reprintform>

To subscribe to BMJ go to:

<http://group.bmj.com/subscribe/>